The Abdus Salam
International Centre for Theoretical Physics

United Nations
Educational, Scientific
and Cultural Organization

International Atomic
Energy Agency

SMR 1773 - 5

SCHOOL ON PHYSICS AT LHC: "EXPECTING LHC"
11 - 16 September 2006

QCD at the LHC - Part II

Michelangelo L. MANGANO
C.E.R.N. - Theory Division, Department of Physics
CH-1211 Geneva 23, Switzerland

Strada Costiera 11, 34014 Trieste, Italy - Tel. +39 040 2240 111; Fax +39 040 224 163 - sci_info@ictp.it, www.ictp.it

QCD at the LHC

ICTP, Trieste, Sept 12-13 2006

LECTURE II

Michelangelo L. Mangano
TH Unit, Physics Dept, CERN
michelangelo.mangano@cern.ch

Drell-Yan processes

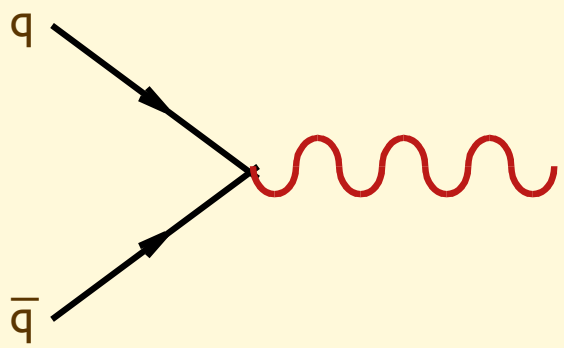

$$W \to \ell\nu$$
$$Z \to \ell^+\ell^-$$

Properties/Goals of the measurement:

- Clean final state (no hadrons from the hard process)
- Tests of QCD: σ(W,Z) known up to NNLO (2-loops)
- Measure m(W) (➙ constrain m(H))
- constrain PDFs (e.g. $f_{up}(x)/f_{down}(x)$)
- search for new gauge bosons:
- Probe contact interactions:

$$q\bar{q} \to W', Z'$$
$$q\bar{q}\ell^+\ell^-$$

LO Cross-section calculation

$$\sigma(pp \to W) = \sum_{q,q'} \int dx_1 dx_2 \, f_q(x_1, Q) \, f_{\bar{q}'}(x_2, Q) \, \frac{1}{2\hat{s}} \int d[PS] \overline{\sum_{spin,col}} |M(q\bar{q}' \to W)|^2$$

where:

$$\overline{\sum_{spin,col}} |M(q\bar{q}' \to W)|^2 = \frac{1}{3}\frac{1}{4} 8 g_W^2 |V_{qq'}|^2 \hat{s} = \frac{2}{3}\frac{G_F m_W^2}{\sqrt{2}} |V_{qq'}|^2 \hat{s}$$

$$d[PS] = \frac{d^3 p_W}{(2\pi)^3 p_W^0} (2\pi)^4 \delta^4(P_{in} - p_W)$$
$$= 2\pi d^4 p_W \, \delta(p_W^2 - m_W^2) \, \delta^4(P_{in} - p_W) = 2\pi \delta(\hat{s} - m_W^2)$$

leading to:

$$\sigma(pp \to W) = \sum_{ij} \frac{\pi A_{ij}}{m_W^2} \tau \int_\tau^1 \frac{dx}{x} f_i(x, Q) \, f_j(\frac{\tau}{x}, Q) \equiv \sum_{ij} \frac{\pi A_{ij}}{m_W^2} \tau L_{ij}(\tau)$$

where:

$$\frac{\pi A_{u\bar{d}}}{m_W^2} = 6.5\text{nb} \quad \text{and} \quad \tau = \frac{m_W^2}{S}$$

Study the function τL(τ)

Assume, for example, that $f(x) \sim \frac{1}{x^{1+\delta}}, \quad 0 < \delta < 1$

Then: $L(\tau) = \int_\tau^1 \frac{dx}{x} \frac{1}{x^{1+\delta}} (\frac{x}{\tau})^{1+\delta} = \frac{1}{\tau^{1+\delta}} \log(\frac{1}{\tau})$

and: $\sigma_W = \sigma_W^0 \left(\frac{S}{m_W^2}\right)^\delta \log\left(\frac{S}{m_W}\right)$

Therefore the W cross-section grows at least logarithmically with the hadronic CM energy. This is a typical behavior of cross-sections for production of fixed-mass objects in hadronic collisions, contrary to the case of e+e- collisions, where cross-sections tend to decrease with CM energy.

Note also the following relation, which allows the measurement of the total width of the W boson from the determination of the leptonic rates of W and Z bosons,

$$\Gamma_W = \frac{N(e^+e^-)}{N(e^\pm\nu)} \left(\frac{\sigma_{W^\pm}}{\sigma_Z}\right) \left(\frac{\Gamma^W_{e\nu}}{\Gamma^Z_{e^+e^-}}\right) \Gamma_Z$$

LHC data — theory — LEP/SLC

PDF luminosity uncertainties

At the Tevatron

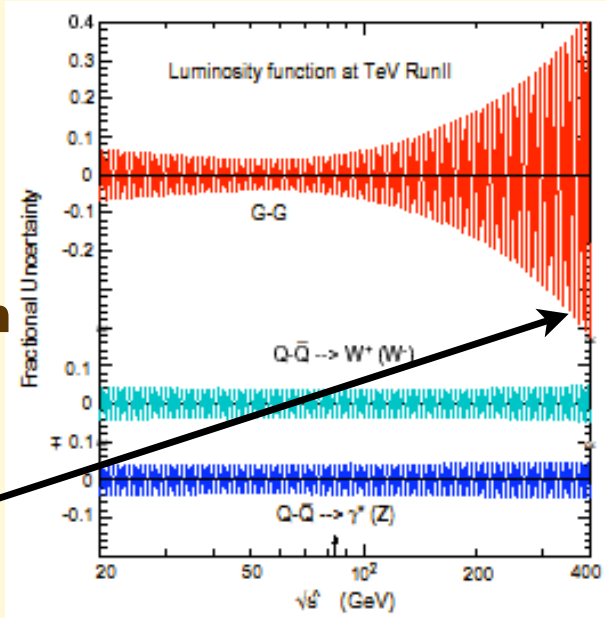

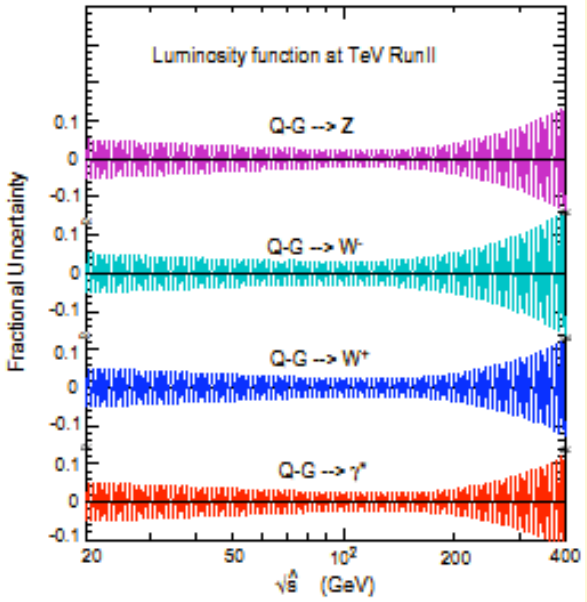

tt production, smaller uncertainty at the LHC!

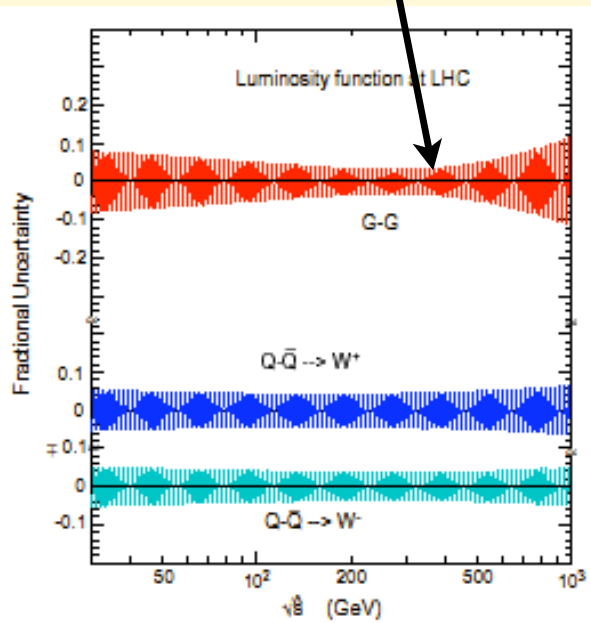

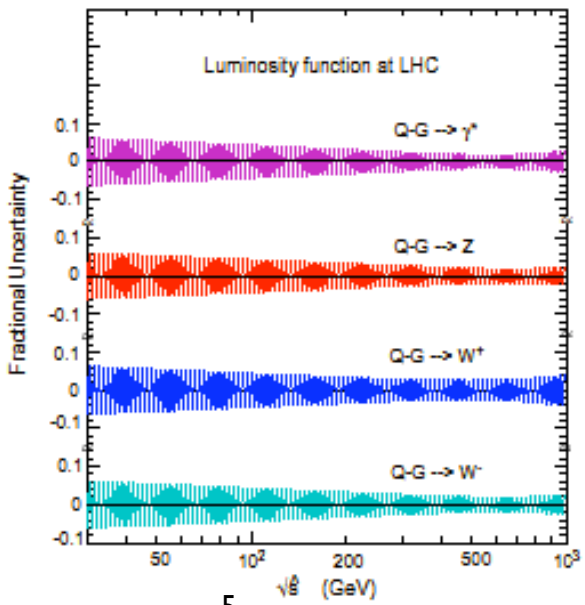

At the LHC

Some useful relations and definitions

Rapidity: $y = \frac{1}{2} \log \frac{E_W + p_W^z}{E_W - p_W^z}$

Pseudorapidity: $\eta = -\log(\tan\frac{\theta}{2})$

where:

$\tan\theta = \frac{p_T}{p^z}$ and $p_T = \sqrt{p_x^2 + p_y^2}$

Exercise: prove that for a massless particle rapidity=pseudorapidity:

Exercise: using $\tau = \frac{\hat{s}}{S} = x_1 x_2$ and

$$\begin{cases} E_W = (x_1 + x_2) E_{beam} \\ p_W^z = (x_1 - x_2) E_{beam} \end{cases} \Rightarrow y = \frac{1}{2} \log \frac{x_1}{x_2}$$

prove the following relations:

$$x_{1,2} = \sqrt{\tau} e^{\pm y} \qquad dx_1\, dx_2 = dy\, d\tau$$

$$dy = \frac{dx_1}{x_1} \qquad d\tau\, \delta(\hat{s} - m_W^2) = \frac{1}{S}$$

Jets in hadronic collisions

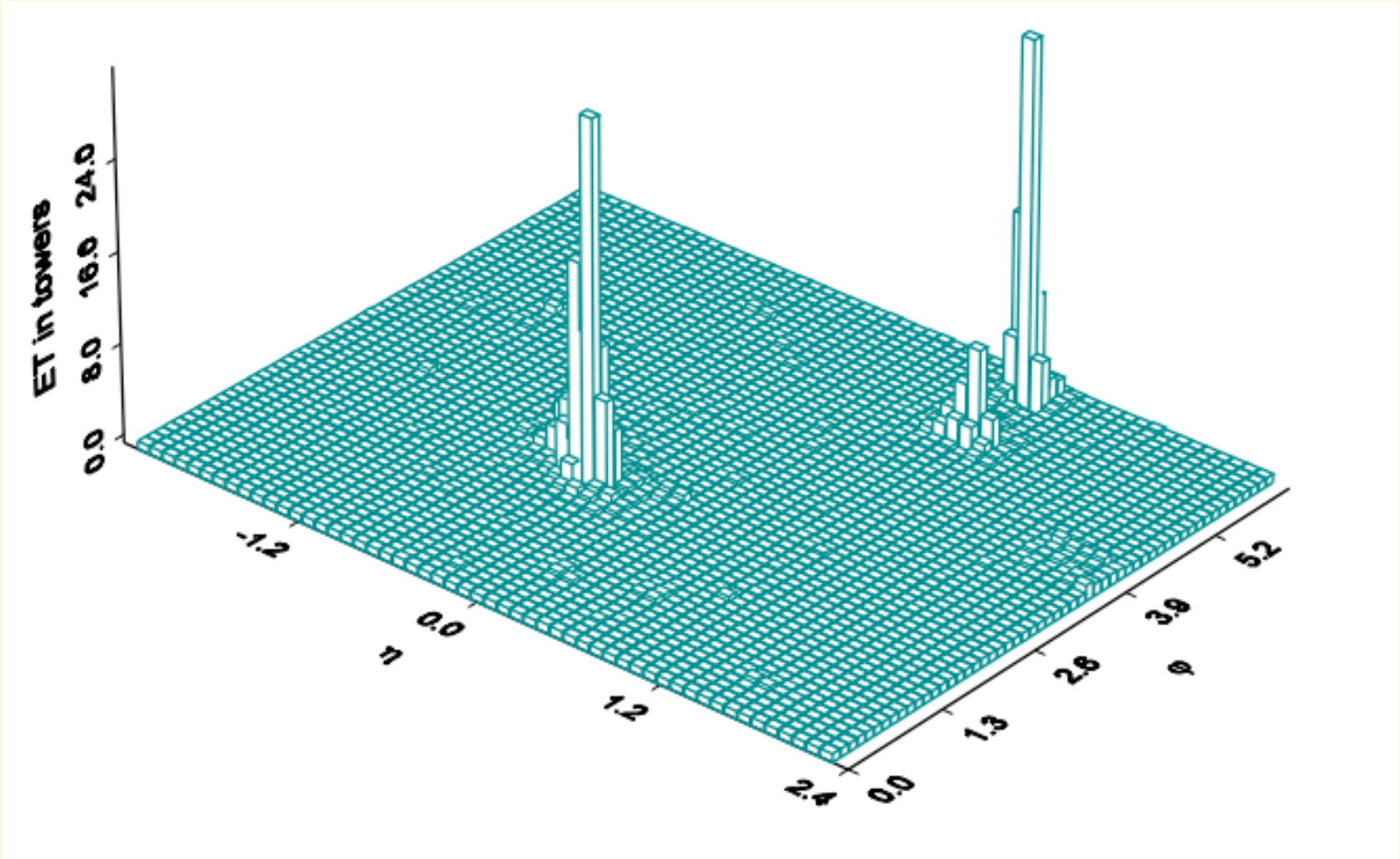

- Inclusive production of jets is the largest component of high-Q phenomena in hadronic collisions
- QCD predictions are known up to NLO accuracy
- Intrinsic theoretical uncertainty (at NLO) is approximately 10%
- Uncertainty due to knowledge of parton densities varies from 5-10% (at low transverse momentum, p_T to 100% (at very high p_T, corresponding to high-x gluons)
- Jet are used as probes of the quark structure (possible substructure implies departures from point-like behaviour of cross-section), or as probes of new particles (peaks in the invariant mass distribution of jet pairs)

$gg \to gg$

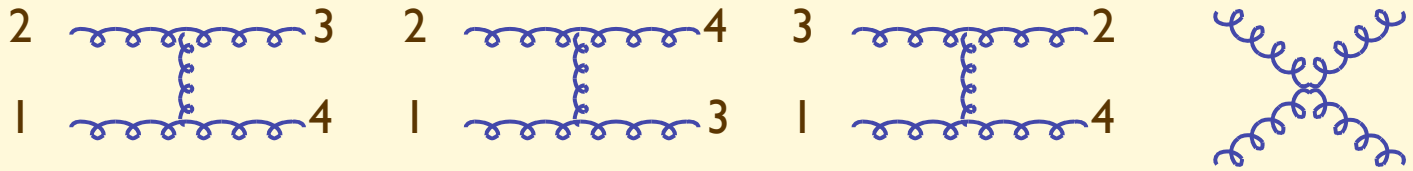

$gg \to q\bar{q}$

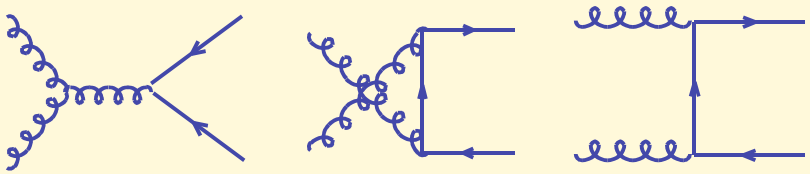

$qg \to qg$

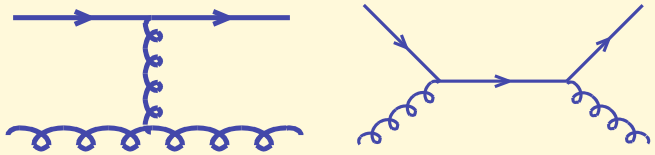

$q\bar{q} \to gg$

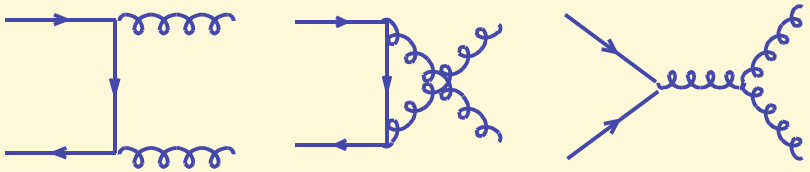

$qq' \to qq'$

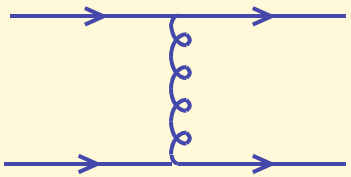

$q\bar{q} \to q\bar{q}$

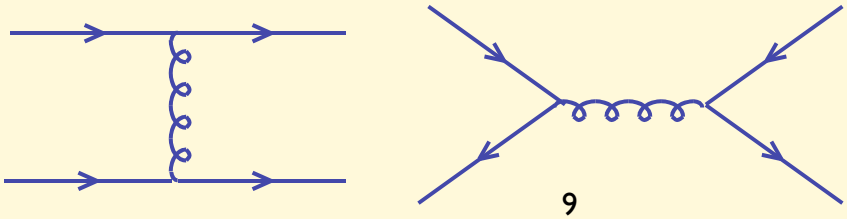

Phase space and cross-section for LO jet production

$$d[PS] = \frac{d^3p_1}{(2\pi)^2 2p_1^0}\frac{d^3p_2}{(2\pi)^2 2p_2^0}(2\pi)^4\delta^4(P_{in}-P_{out})\,dx_1\,dx_2$$

(a) $$\delta(E_{in}-E_{out})\,\delta(P_{in}^z-P_{out}^z)\,dx_1\,dx_2 = \frac{1}{2E_{beam}^2}$$

(b) $$\frac{dp^z}{p^0} = dy \equiv d\eta$$

$$d[PS] = \frac{1}{4\pi S}\,p_T\,dp_T\,d\eta_1\,d\eta_2$$

$$\frac{d^3\sigma}{dp_T d\eta_1 d\eta_2} = \frac{p_T}{4\pi S}\sum_{i,j} f_i(x_1)\,f_j(x_2)\,\frac{1}{2\hat{s}}\overline{\sum_{kl}}\,|M(ij\to kl)|^2$$

The measurement of pT and rapidities for a dijet final state uniquely determines the parton momenta x_1 and x_2. Knowledge of the partonic cross-section allows therefore the determination of partonic densities f(x)

Small-angle jet production, a useful approximation for the determination of the matrix elements and of the cross-section

At small scattering angle, $t = (p_1 - p_3)^2 \sim (1 - \cos\theta) \to 0$

and the $1/t^2$ propagators associated with t-channel gluon exchange dominate the matrix elements for all processes. In this limit it is easy to evaluate the matrix elements. For example:

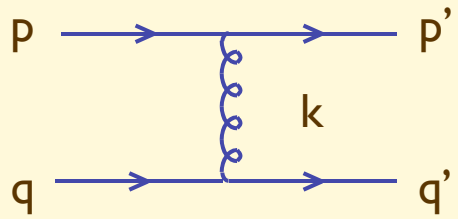

$$\sim (\lambda^a)_{ij}(\lambda^a)_{kl}(2p_\mu)\frac{1}{t}(2q_\mu) = \frac{2s}{t}(\lambda^a)_{ij}(\lambda^a)_{kl}$$

where we used the fact that, for k=p-p'<<p (small angle scattering),

$$\bar{u}(p')\gamma_\mu u(p) \sim \bar{u}(p)\gamma_\mu u(p) = 2p_\mu$$

Using our colour algebra results, we then get: $\overline{\sum_{col,spin}} |M|^2 = \frac{1}{N_c^2}\frac{N_c^2-1}{4}\frac{4s^2}{t^2}$

Noting that the result must be symmetric under s↔u exchange, and setting Nc=3, we finally obtain: $\overline{\sum_{col,spin}} |M|^2 = \frac{4}{9}\frac{s^2+u^2}{t^2}$

which turns out to be the exact result!

Quark-gluon and gluon-gluon scattering

We repeat the exercise in the more complex case of qg scattering, assuming the dominance of the t-channel gluon-exchange diagram:

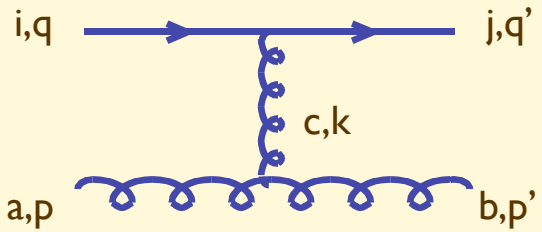

$$\sim f^{abc}\lambda^c_{ij}\,2p_\mu\frac{1}{t}2q_\mu = 2\frac{s}{t}f^{abc}\lambda^c_{ij}$$

Using the colour algebra results, and enforcing the s↔u symmetry, we get:

$$\overline{\sum_{col,spin}}|M|^2 = \frac{s^2+u^2}{t^2}$$

which differs by only 20% from the exact result

$$\overline{\sum_{col,spin}}|M|^2 = \frac{s^2+u^2}{t^2} - \frac{4}{9}\frac{s^2+u^2}{us}$$

even in the large-angle region, at 90°

In a similar way we obtain for gg scattering (using the t↔u symmetry):

$$\overline{\sum_{col,spin}}|M(gg\to gg)|^2 = \frac{9}{2}\left(\frac{s^2}{t^2}+\frac{s^2}{u^2}\right)$$

compared to the exact result

$$\overline{\sum_{col,spin}}|M(gg\to gg)|^2 = \frac{9}{2}\left(3-\frac{ut}{s^2}-\frac{us}{t^2}-\frac{st}{u^2}\right)$$

with a 20% difference at 90°

Note that in the leading 1/t approximation we get the following result:

$$\hat{\sigma}_{gg} : \hat{\sigma}_{qg} : \hat{\sigma}_{qq} = \frac{9}{4} : 1 : \frac{4}{9}$$

where 4/9 = C_F / C_A = [(N^2-1)/2N] / N is the ratio of the squared colour charges of quarks and gluons

and therefore

$$d\sigma_{jet} = \int dx_1\, dx_2 \sum_{ij} f_i(x_1)\, f_j(x_2)\, d\hat{\sigma}_{ij} = \int dx_1\, dx_2 \sum_{ij} F(x_1)\, F(x_2)\, d\hat{\sigma}_{gg}$$

where we defined the `effective parton density' F(x):

$$F(x) = g(x) + \frac{4}{9} \sum_i [q_i(x) + \bar{q}_i(x)]$$

As a result jet data cannot be used to extract separately gluon and quark densities. On the other hand, assuming an accurate knowledge of the quark densities (say from HERA), jet data can help in the determination of the gluon density

Process	$\frac{d\hat{\sigma}}{d\Phi_2}$	at 90°
$qq' \to qq'$	$\frac{4}{9}\frac{\hat{s}^2+\hat{u}^2}{\hat{t}^2}$	2.22
$qq \to qq$	$\left[\frac{4}{9}\left(\frac{\hat{s}^2+\hat{u}^2}{\hat{t}^2}+\frac{\hat{s}^2+\hat{t}^2}{\hat{u}^2}\right)-\frac{8}{27}\frac{\hat{s}^2}{\hat{u}\hat{t}}\right]$	3.26
$q\bar{q} \to q'\bar{q}'$	$\frac{4}{9}\frac{\hat{t}^2+\hat{u}^2}{\hat{s}^2}$	0.22
$q\bar{q} \to q\bar{q}$	$\left[\frac{4}{9}\left(\frac{\hat{s}^2+\hat{u}^2}{\hat{t}^2}+\frac{\hat{t}^2+\hat{u}^2}{\hat{s}^2}\right)-\frac{8}{27}\frac{\hat{u}^2}{\hat{s}\hat{t}}\right]$	2.59
$q\bar{q} \to gg$	$\left[\frac{32}{27}\frac{\hat{t}^2+\hat{u}^2}{\hat{t}\hat{u}}-\frac{8}{3}\frac{\hat{t}^2+\hat{u}^2}{\hat{s}^2}\right]$	1.04
$gg \to q\bar{q}$	$\left[\frac{1}{6}\frac{\hat{t}^2+\hat{u}^2}{\hat{t}\hat{u}}-\frac{3}{8}\frac{\hat{t}^2+\hat{u}^2}{\hat{s}^2}\right]$	0.15
$gq \to gq$	$\left[-\frac{4}{9}\frac{\hat{s}^2+\hat{u}^2}{\hat{s}\hat{u}}+\frac{\hat{u}^2+\hat{s}^2}{\hat{t}^2}\right]$	6.11
$gg \to gg$	$\frac{9}{2}\left(3-\frac{\hat{t}\hat{u}}{\hat{s}^2}-\frac{\hat{s}\hat{u}}{\hat{t}^2}-\frac{\hat{s}\hat{t}}{\hat{u}^2}\right)$	30.4

Some more kinematics

Prove as an **exercise** that

$$x_{1,2} = \frac{p_T}{E_{beam}} \cosh y^* \, e^{\pm y_b}$$

where

$$y^* = \frac{\eta_1 - \eta_2}{2}, \quad y_b = \frac{\eta_1 + \eta_2}{2}$$

We can therefore reach large values of x either by selecting large invariant mass events:

$$\frac{p_T}{E_{beam}} \cosh y^* \equiv \sqrt{\tau} \to 1$$

or by selecting low-mass events, but with large boosts (y_b large) in either positive of negative directions. In this case, we probe large-x with events where possible new physics is absent, thus setting consistent constraints on the behaviour of the cross-section in the high-mass region, which could hide new phenomena.

Example, at the Tevatron

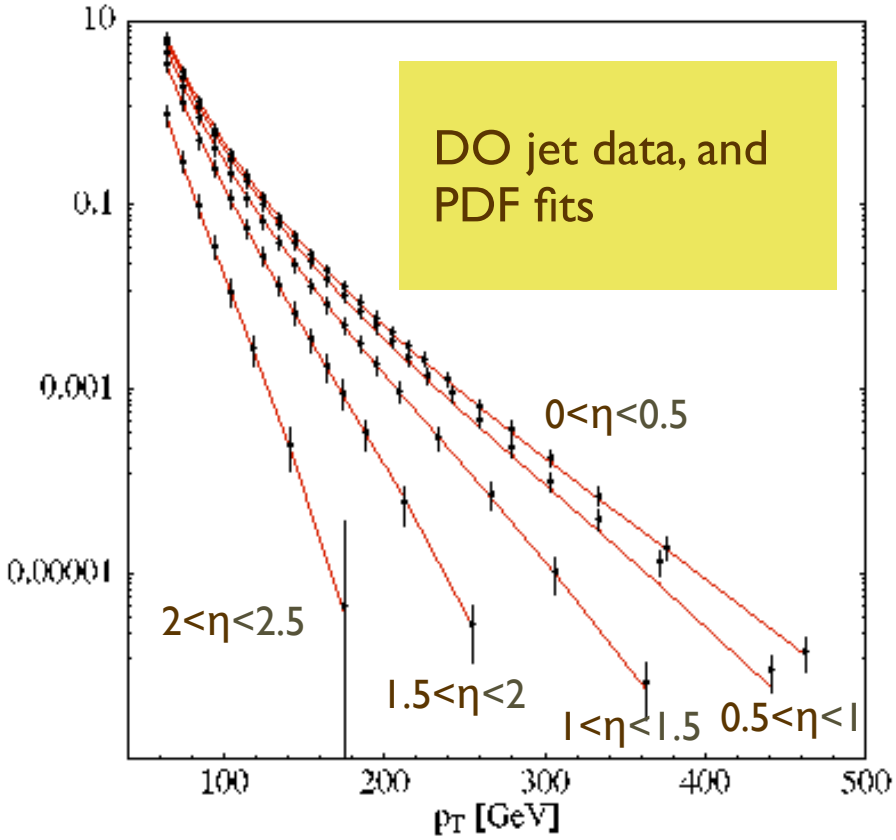

DO jet data, and PDF fits

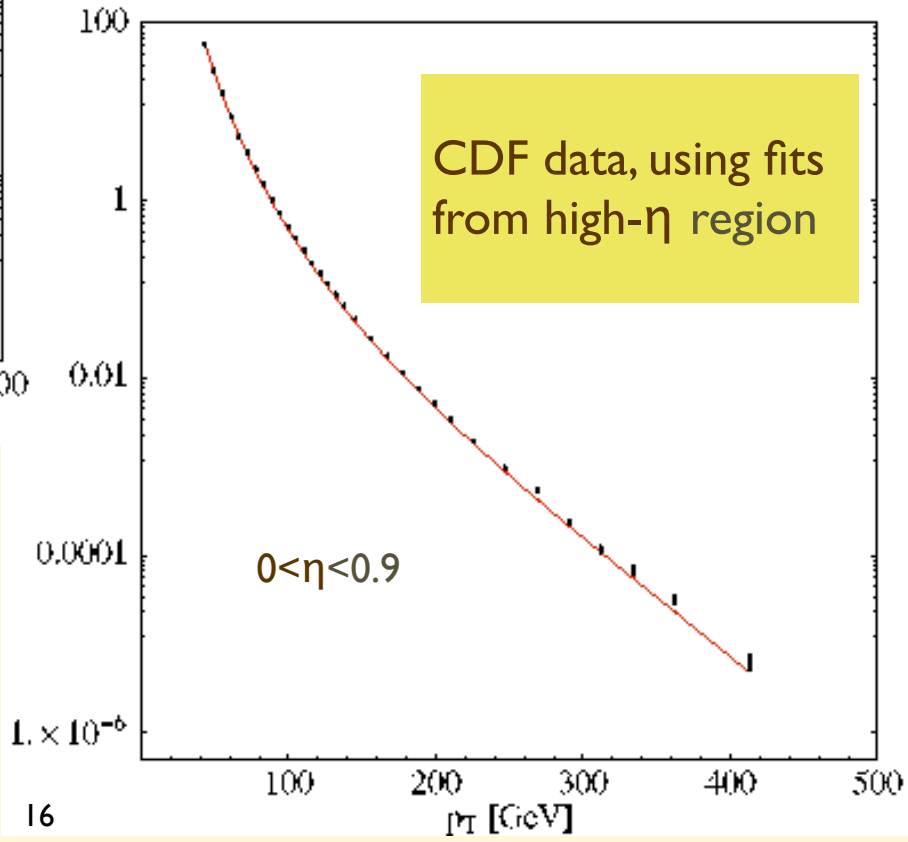

CDF data, using fits from high-η region

Multijet rates

σ [μb]	N jet=2	N jet=3	N jet=4	N jet=5
E_T^{jet} >20 GeV	350	19	2.6	0.35
E_T^{jet} >50 GeV	12.7	0.45	0.045	0.004
E_T^{jet} >100 GeV	0.85	0.021	0.0015	0.0001

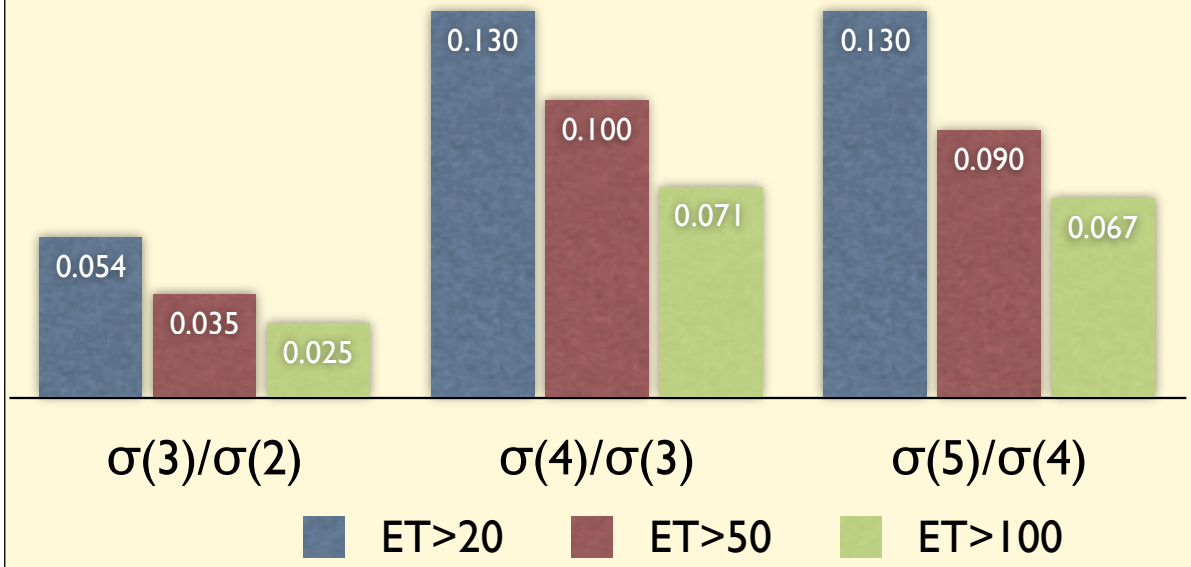

- The higher the jet E_T threshold, the harder to emit an extra jet
- When several jets are already present, however, emission of an additional one is less suppressed

Multijet rates, vs $\sqrt{s}$, with $E_T^{jet} > 20$ GeV

σ [μb]	N jet=2	N jet=3	N jet=4	N jet=5
$\sqrt{s} > 100$ GeV	75	17.3	2.6	0.37
$\sqrt{s} > 500$ GeV	0.27	0.47	0.30	0.13
$\sqrt{s} > 1000$ GeV	0.012	0.021	0.022	0.031

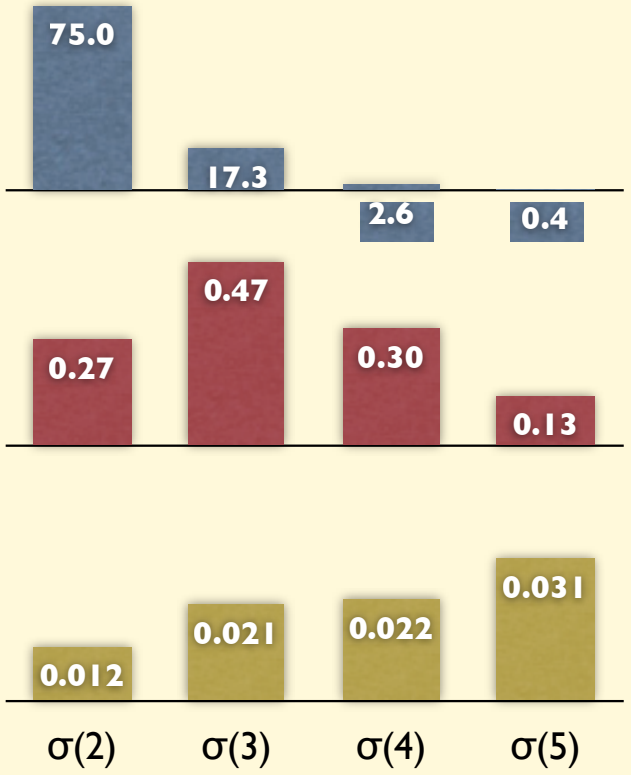

High mass final states are dominated by multijet configurations

W+Multijet rates

σxB(W→eν)[pb]	N jet=1	N jet=2	N jet=3	N jet=4	N jet=5	N jet=6
LHC	3400	1130	340	100	28	7
Tevatron	230	37	5.7	0.75	0.08	0.009

E_T(jets) > 20 GeV , $|\eta|$<2.5 , ΔR>0.7

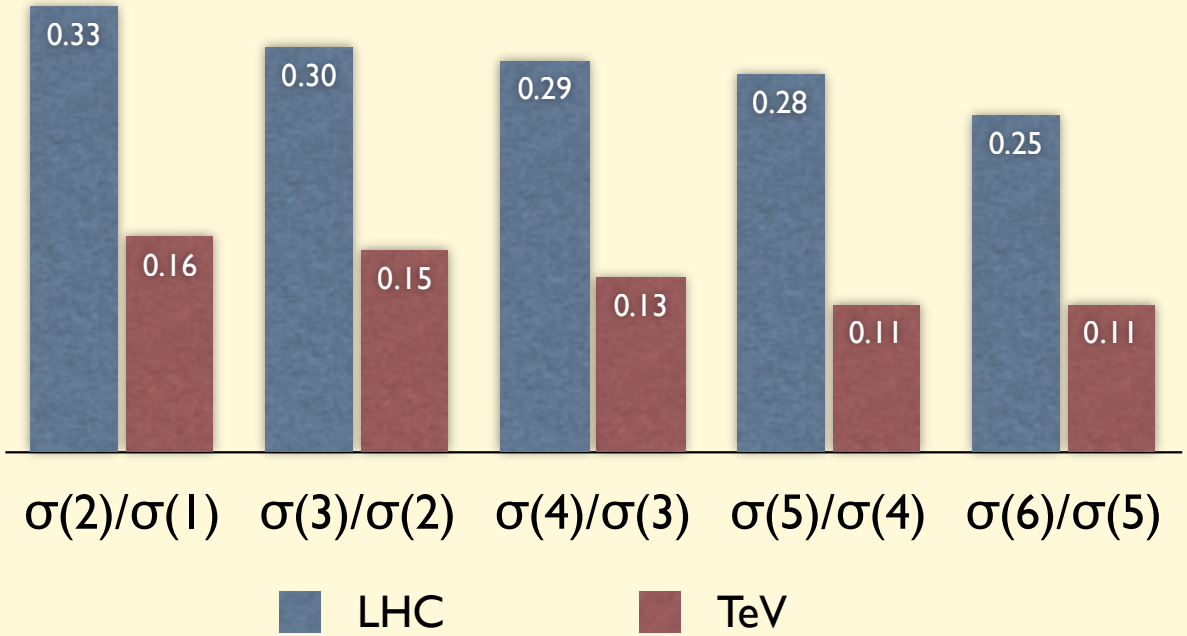

- Ratios almost constant over a large range of multiplicities
- $O(\alpha_s)$ at Tevatron, but much bigger at LHC

Wbb+jets rates

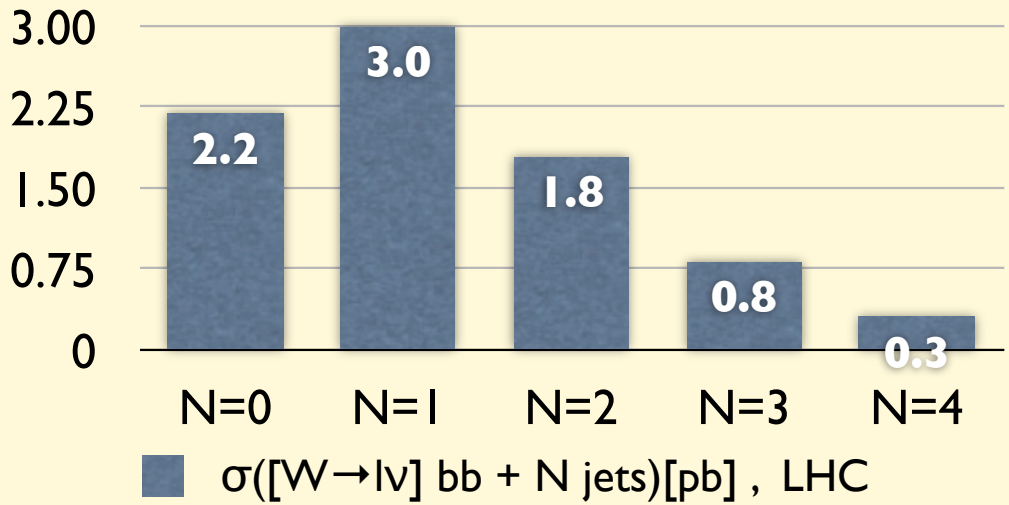

Pattern of multiplicity distribution very different than in W+jets!

In pp collisions (contrary to the Tevatron, p-pbar) :

$N_{jet}=0 \propto \alpha_s^2 \times \text{Lum}(q\ \text{qbar}) \approx N_{jet}=1 \propto \alpha_s^3 \times \text{Lum}(q\ g)$

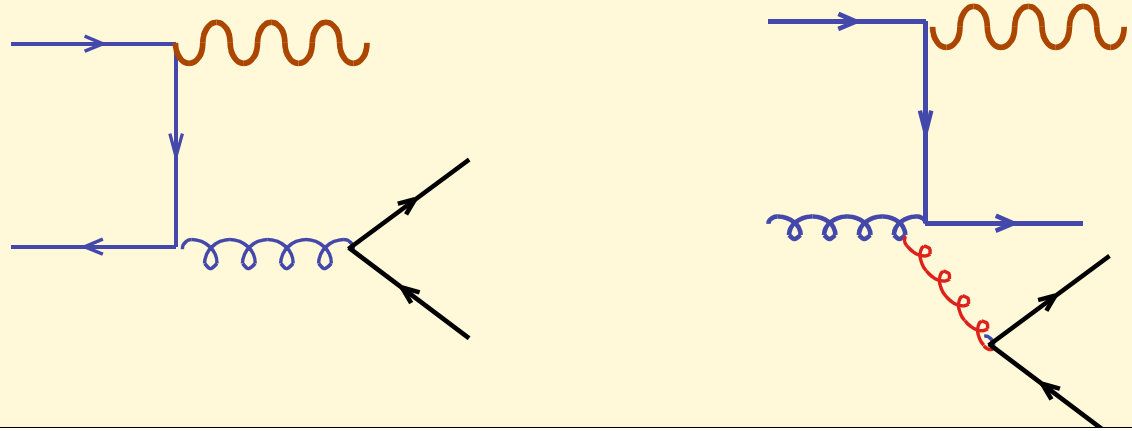

Beware of naive α_s power counting!!

Top production and bgs

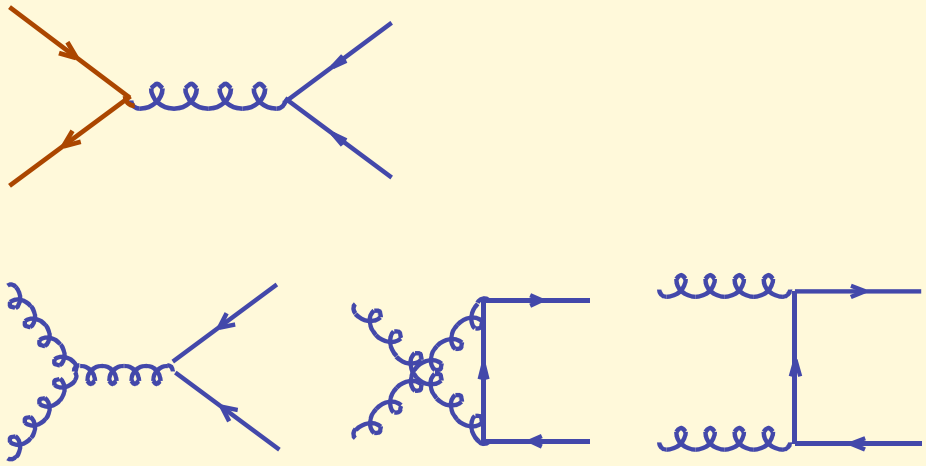

	σ(tt) [pb]	σ(W+X)	σ(W+bbX) [ptb>20 GeV]	σ(W+bbjj X) [ptb,ptj >20 GeV]
Tevatron	6	20×10^3	3	0.16
LHC	800	160×10^3	20	16
Increase	x 100	x 10	x 10	x 100

Missing E_T > 20 GeV
1 lepton P_T > 20 GeV
4 jets(R=0.4) P_T > 40 GeV

No b-tagging required

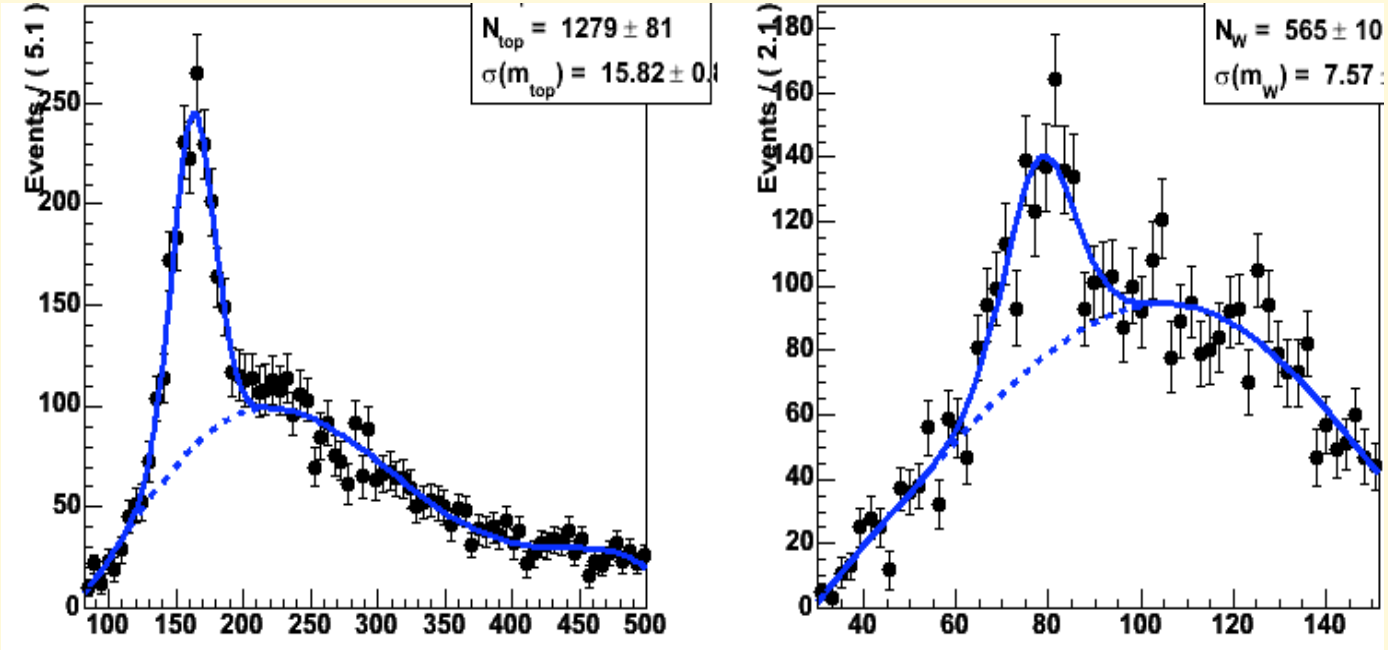

The signal is clearly visible over the background, even without b tagging

tt cross-section

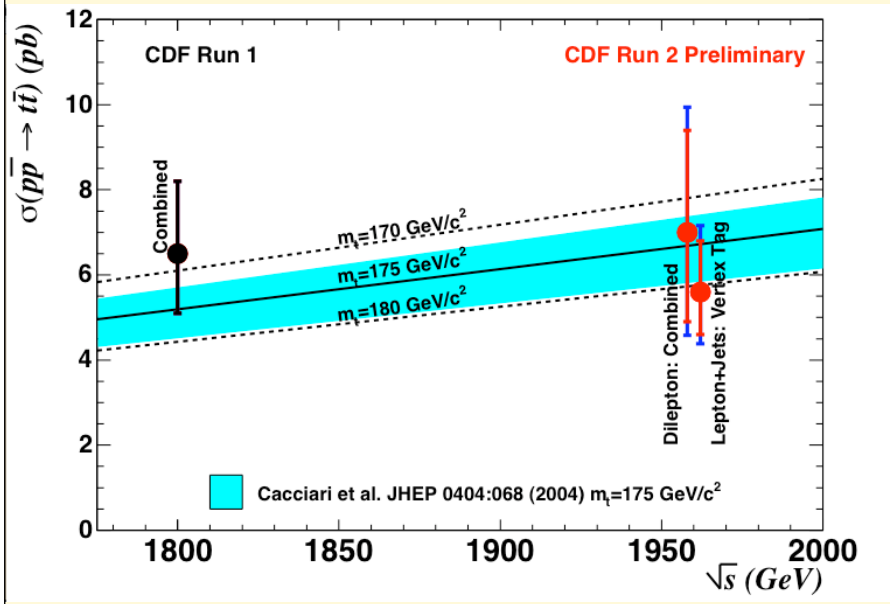

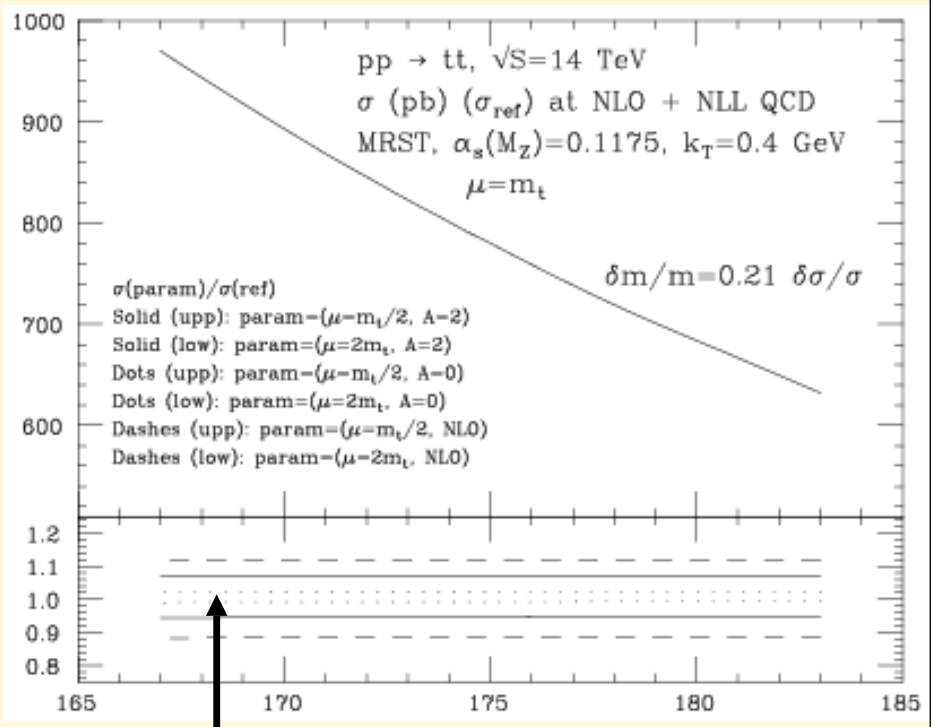

$\sigma_{tt}^{FNAL} = 6.5pb\ (1 \pm 5\%_{scale} \pm 7\%_{PDF})$

$\sigma_{tt}^{LHC} = 840pb\ (1 \pm 5\%_{scale} \pm 3\%_{PDF})$

Scale unc: $\pm\ 12\%_{NLO} \Rightarrow \pm\ 5\%_{NLO+NLL}$)

$\Delta\sigma = \pm\ 6\% \Rightarrow \Delta m = \pm\ 2$ GeV

Leptons

Experimentally, electrons, muons and taus are entirely different objects. Their identification requires different components of the detector, different techniques, and is subject to different backgrounds.

As seen from a theorists, all leptons are produced the same. Nevertheless there is a large variety of possible production mechanisms, each one of them leading to different overall properties of the final state. When considering leptons as a signal for new physics, it is important to have a clear picture of their irreducible SM sources

Single lepton

Sources of single high-pt leptons:

- $W \rightarrow e/\mu + \nu$
- $Z \rightarrow \tau\tau \rightarrow e/\mu + X$
- $b \rightarrow e/\mu + X$
- $t \rightarrow Wb \rightarrow e/\mu + \nu + b$

Differential Rates

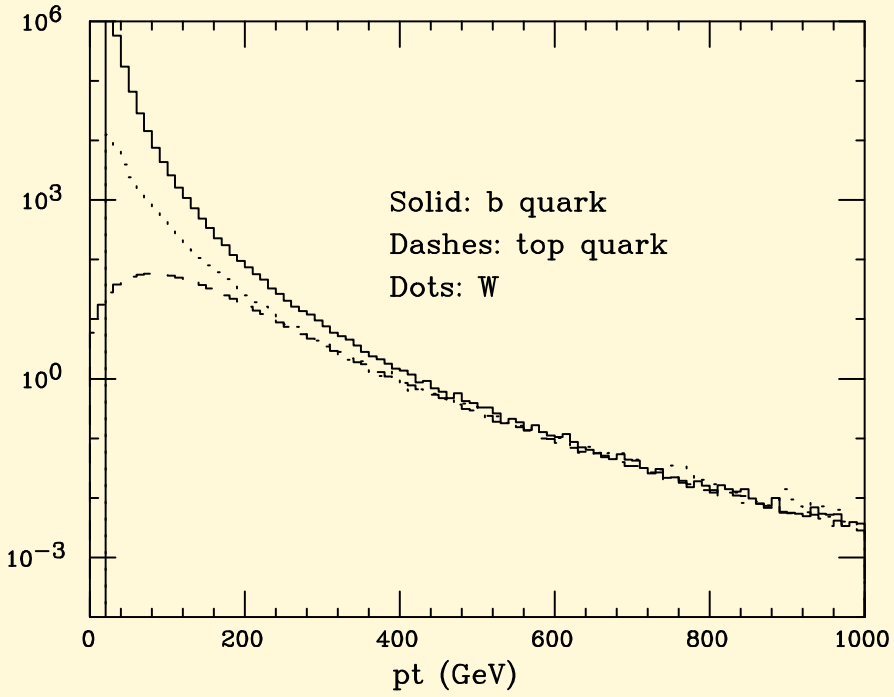

- At large pt b and t production ~ equal !
- At large pt, W and heavy quark production ~ equal!

*W → lepton is a 2-body decay, b/t → lepton is 3-body: lepton takes a larger fraction of momentum in W decay => harder spectrum, larger rate at higher pt in W production

*The global features of the event accompanying the lepton will clearly be very different in each case. Which of the three processes will dominate in a given analisys, will therefore depend on the details

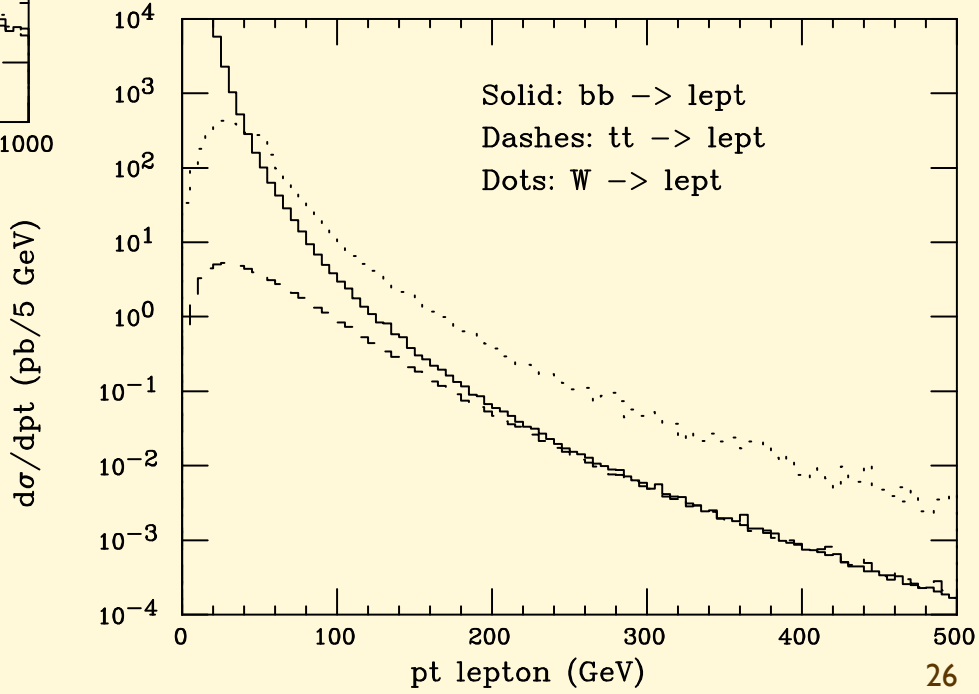

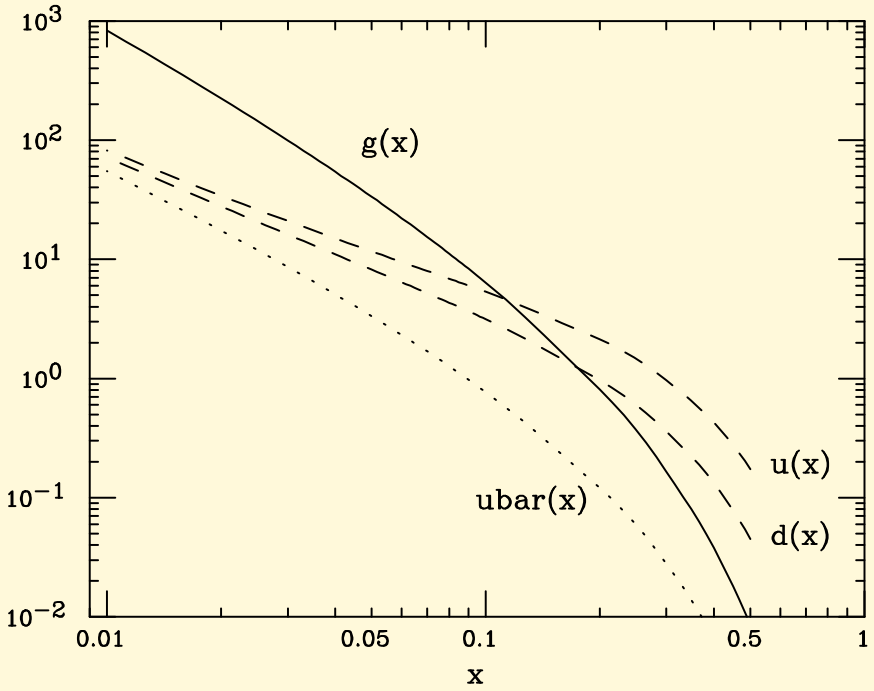

How come Q and W spectra are comparable at large Et?

The LO processes for QQ production are weighted by the gg or qqbar luminsity, which drops at large mass much more rapidly than L(qg)

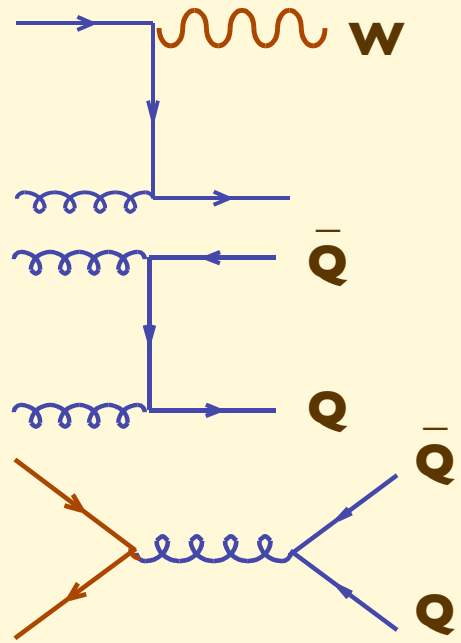

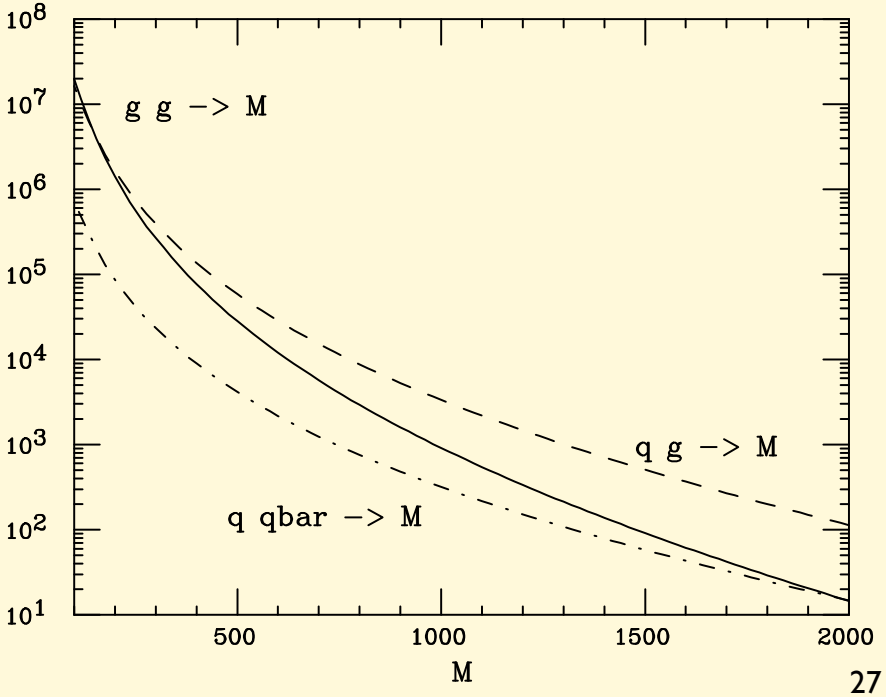

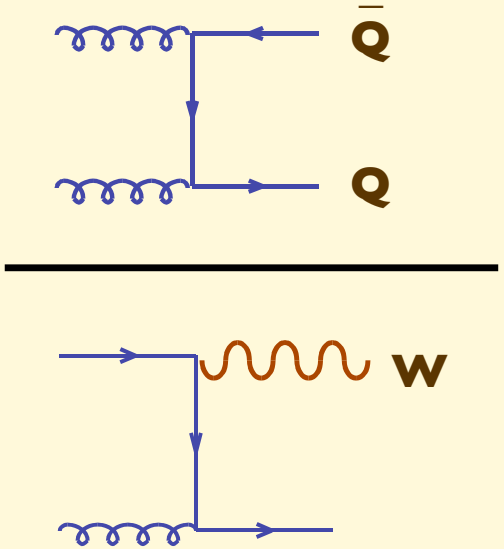

$$=$$

Quark colour charge

Initial state colour averages

~1/3 at 90°

$$\frac{C_F \alpha_s}{1/2 \times \alpha_w} \times \left(\frac{N}{N^2-1}\right) \times \frac{1}{1/2} \times F(s \leftrightarrow u)$$

Quark weak charge

V-A, only L-handed quarks

$$\approx \quad \frac{\alpha_s}{\alpha_W} \sim 3$$

Dileptons

One lepton W: 160 nb

WW	tt	Z
75pb	500pb	50nb
2l+MET, no jets	2l+MET, jets, b's	2l, m(ll)=mZ, no MET, no jets

Dilepton production dominated by top pairs!

Trileptons

WWW	ttW	ZW
130fb	500fb	28pb

ttW ~ 10^{-3} tt => trilepton contribution from tt, with 3rd lepton form b→l decay, important => require isolation!

Quadrileptons

WWWW	tttt	ZWW
0.6fb	12fb	100fb

ZWWW=0.7fb

Ratios

W/Z	WW / WZ	WWW / WWZ	WWWW / WWWZ
3	2.5	1.3	1

Ratio determined by couplings to quarks, u/d asymmetry of proton

Ratio determined by couplings among W/Z, SU(2) invariance

WW/W	WWW / WW	WWWW / WWW
.5E-3	2E-3	5e-3

ZW / W	ZWW / WW	ZWWW / WWW
.5E-3	4E-3	7e-3

1W
~10^{-3}